

1 **Differentiating local and regional sources of Chinese urban air pollution based on**  
2 **effect of Spring Festival**

3

4 Chuan Wang, Xiao-Feng Huang\*, Qiao Zhu, Li-Ming Cao, Bin Zhang, Ling-Yan He

5

6 Key Laboratory for Urban Habitat Environmental Science and Technology, School of Environment and Energy,  
7 Peking University Shenzhen Graduate School, Shenzhen, 518055, China.

8

9 \*Corresponding author: [huangxf@pku.edu.cn](mailto:huangxf@pku.edu.cn)

10

11 **Abstract:** The emission of pollutants is extremely reduced during the annual Chinese Spring Festival  
12 (SF) in Shenzhen, China. During the SF, traffic flow drops by ~50% and the industrial plants are almost  
13 entirely shut down in Shenzhen. To characterize the variation in ambient air pollutants due to the  
14 “Spring Festival effect”, various gaseous and particulate pollutants were measured in real time in urban  
15 Shenzhen over three consecutive winters (2014–2016). The results indicate that the concentrations of  
16 NO<sub>x</sub>, volatile organic compounds (VOCs), black carbon (BC), primary organic aerosols, chloride, and  
17 nitrate in submicron aerosols decrease by 50%–80% during the SF period relative to the non-Spring  
18 Festival periods, regardless of meteorological conditions, which suggests that these pollutants are  
19 mostly emitted or secondarily formed from urban local emissions. The concentration variation of  
20 species mostly from regional or natural sources, however, is found to be much less, such as for bulk  
21 PM<sub>2.5</sub>. More detailed analysis of the Spring Festival effect reveals an urgent need to reduce emissions  
22 of SO<sub>2</sub> and VOCs on a regional scale rather than on an urban scale to reduce urban PM<sub>2.5</sub> in Shenzhen,  
23 which can also produce some use for reference for other megacities in China.

24 **Key words:** Spring Festival effect; local emissions; regional pollution; PM<sub>2.5</sub>; ozone

## 25 **1 Introduction**

26 The rapid economic development and urbanization of China over the recent decades has brought with  
27 it the consequence of severe atmospheric pollution, especially in the key economically developed  
28 regions, such as the Beijing–Tianjin–Hebei region (Sun et al., 2013, 2015; Guo et al., 2014), the  
29 Yangtze River Delta (Huang et al., 2013), and the Pearl River Delta (PRD), as well as their densely  
30 populated megacities (Hagler et al., 2006; Zhang et al., 2008; He et al., 2011). Great efforts have been  
31 made to determine the sources and formation mechanisms of fine particles (PM<sub>2.5</sub>) in these region.  
32 Previous studies indicate that PM<sub>2.5</sub> forms from primary fine particles and through secondary formation  
33 from gaseous precursors (Zhang et al., 2008; Zheng et al., 2009a; Huang et al., 2014), and the sources  
34 of local production and regional transport are both important (Huang et al., 2014; Huang et al., 2006,  
35 2011; Li et al., 2015).

36  
37 The causes of air pollution in urban atmosphere in China are particularly complicated, and bring great  
38 challenges to management strategies for protecting human health (Parrish and Zhu, 2009). To explore  
39 the causes of urban air pollution in China, previous studies have focused on monitoring and comparing  
40 the reduction in emissions during special events, such as the 2008 Beijing Olympic Games (Huang et  
41 al., 2010), the 2010 Guangzhou Asian Games (Xu et al., 2013), the 2014 Asia Pacific Economic  
42 Cooperation conference (APEC) (Chen et al., 2015; Sun et al., 2016; Zhang et al., 2016) and the 2015  
43 China victory day parade (Zhao et al., 2016). During such events, the air quality improved remarkable  
44 because of short-term limitations on traffic and industrial activity (Huang et al., 2010; Wang et al.,  
45 2010; Xu et al., 2013; Sun et al., 2016; Zhao et al., 2016). However, these limitations were temporary,  
46 non-repeatable measures, so the air quality monitoring campaigns cannot be repeated. Actually, a

47 spontaneous reduction in emissions occurs every year in China during the Spring Festival (SF), which  
48 is the single most important holiday in China. During the week-long holiday (in January or February  
49 every year), the urban emission patterns depart significantly from the usual patterns: traffic decreases  
50 in the mega cities because most people are not working, and most of the industries, stores, and  
51 production sites are closed in the city except for the infrastructure (e.g., power plants) that cannot be  
52 shut down (Qin et al., 2004; Feng et al., 2012; Shi et al., 2014). Tan et al. (2009) reported that the  
53 concentrations of NO<sub>x</sub>, CO, NMHC, SO<sub>2</sub>, and PM<sub>10</sub> were lower in the SF periods than in the non-  
54 Spring Festival (NSF) periods in the metropolitan area of Taipei over 1994-2006, while the variation  
55 of O<sub>3</sub> was in a reversed trend. Jiang et al. (2015) found that the ambient concentrations of VOCs had  
56 a sharp decline by ~60% during the SF in Shijiazhuang.

57

58 This study focuses on Shenzhen as a special example to evaluate the effect on urban air pollution of  
59 the SF. Shenzhen is in the eastern Pearl River Delta (PRD) and is the fourth largest economic center  
60 in China, with a total residential population of over 10 million and a fleet of civilian vehicles of more  
61 than 3.1 million (Shenzhen Yearbook of Statistics, 2015). Known as the country's city of most floating  
62 population, Shenzhen owns 7.4 million immigrants in 2014, which accounts 70% of the city's total  
63 population (Shenzhen Yearbook of Statistics, 2015). During the SF period, over 50% of the residents  
64 in Shenzhen are used to travel back to their hometowns (<http://sz.gov.cn>). It is reported that the traffic  
65 flow in Shenzhen during the SF of 2016 (Feb 7–13) was only the half before the SF period  
66 (<http://sz.gov.cn>). Additionally, industrial activities are almost totally suspended in Shenzhen during  
67 the SF period. To characterize the air quality during such extreme reductions of anthropogenic  
68 activities during the SF period in Shenzhen, various air pollutants in Shenzhen urban areas were

69 comprehensively and systematically monitored in real time in winter for three consecutive years  
70 (2014–2016). The annual SF in Shenzhen thus provides an excellent spontaneous control experiment  
71 for local emissions, which could provide unique and valuable information regarding the sources of  
72 urban air pollution.

73

## 74 **2 Experimental methods**

### 75 **2.1 Monitoring sites and meteorological conditions**

76 The monitoring site (22°36'N, 113°54'E) was on the roof (20 m above ground level) of an academic  
77 building on the campus of Peking University Shenzhen Graduate School (PKUSZ) (Figure S1).  
78 PKUSZ is located in the western urban area of Shenzhen, and there are no significant anthropogenic  
79 pollution sources nearby except a local road ~100 m far from the sampling site. A highly resolved  
80 temporal and spatial emission inventory for PRD indicates that the sampling area is characterized by  
81 lower SO<sub>2</sub> emissions but higher NO<sub>x</sub> and VOCs emissions in comparison with other areas in PRD  
82 (Zheng et al., 2009b). The sampling schedule ran roughly from late January to early March over 2014–  
83 2016, which includes the official SF holiday period and the prior and following periods. Our definition  
84 of the SF period follows that of the statutory public holiday calendar in China, and it is continuous  
85 seven days in each year. While the seven days immediately before or after the holidays are actually the  
86 transition periods between the holidays and normal days (called the Tran. periods hereafter), when  
87 people begin to move from the city (or their hometowns) to their hometowns (or the city), the typical  
88 non-spring festival (NSF) periods are better defined as the 7–14 days close to the SF period (called the  
89 NSFT period hereafter, where T indicates time similar). The specific dates and the average  
90 meteorological parameters are listed in Table 1, and Figure S2 shows wind rose plots. The data in Table

91 I show that the meteorology differs among the SF, NSFT, and Tran. periods. To control for the  
92 influence of meteorology on the evaluation of emissions, we selected another 7-day period each year  
93 when the meteorology is similar to that of the SF period (called the NSF<sub>M</sub> period hereafter, where M  
94 indicates meteorology similar); the detailed parameters are listed in Table 1 and Figure S2. The  
95 meteorological data for the SF period are fairly similar to those of the NSF<sub>M</sub> period, suggesting similar  
96 meteorological conditions.

97

98

99

100

101

102

103

104

105

106

107

108

109

110

111

112

113 **Table 1.** Summary of meteorological conditions at sampling site during the SF, NSFT, NSFM and  
 114 Tran. periods of 2014–2016.

		SF	Tran.	NSFT	NSFM
	2014	Jan 31–Feb 6	Feb 7–Feb 13	Feb 14–Feb 20	Feb 20–Feb 26
Data period	2015	Feb 18–Feb 24	Feb 11–Feb 17	Feb 4–Feb 10	Jan 24–Jan 30
	2016	Feb 7–Feb 13	Feb 14–Feb 20	Feb 21–Feb 27	Feb 27–Mar 4
	Temperature (°C)	19.0±4.7	14.1±5.3	14.1±4.0	18.1±3.8
	RH (%)	68.1 ±17.8	69.3±18.4	64.9±16.7	67.4±14.7
	Wind speed (m s <sup>-1</sup> )	0.88 ±0.57	0.81±0.49	0.83±0.48	0.86±0.55
Meteorological parameters	Dominant wind direction	NW	NW and NE	NW and NE	NW
	Precipitation (mm)	0	0	0	0
	UVA (W m <sup>-2</sup> )	5.4±8.5	2.5±4.3	3.8±6.7	5.0±8.0
	UVB (W m <sup>-2</sup> )	0.24±0.40	0.11±0.25	0.16±0.32	0.22±0.38

## 115 2.2 Instrumentation

116 For the ambient sampling in this study, the measuring instruments were placed in a room on the top  
 117 floor of a four-story teaching building at PKUSZ. A high-sensitivity proton transfer reaction mass  
 118 spectrometer (PTR–MS) (Ionicon Analytik GmbH, Austria) was used to measure the selected volatile  
 119 organic compounds (VOCs). The PTR–MS measured a total of 25 masses in the selected ion mode at

120 a time resolution of 30 s. Background checks were done for 30 of every 300 scan cycles with an  
121 activated charcoal trap at 360 °C, which can remove VOCs from the ambient air without changing  
122 water content. The VOCs reported here (Table S1) may be broadly classified into three categories:  
123 oxygenated VOCs [OVOCs: methanol, acetone, methyl ethyl ketone (MEK), acetaldehyde, and acetic  
124 acid], aromatics (benzene, toluene, styrene, C8 and C9 aromatics), and three types of tracers [isoprene,  
125 acetonitrile, and dimethyl sulfide (DMS)]. The PTR-MS was calibrated every 5 to 7 days by using a  
126 TO15 mixture standard (Air Environmental Inc., US) and permeation tubes (Valco Instruments Co.  
127 Inc., US) (de Gouw and Warneke, 2007).

128

129 An aerodyne high-resolution time-of-flight aerosol mass spectrometer (HR-ToF-AMS) (Aerodyne  
130 Research, US) was deployed to measure non-refractory PM<sub>1</sub> (NR-PM<sub>1</sub>) (Canagaratna et al., 2007) in  
131 the period 2014–2015 with a time resolution of 4 min. An aerosol chemical speciation monitor (ACSM)  
132 (Aerodyne Research, US) was used in 2016 with a dynamic resolution of 10 min. The detailed  
133 description of the ACSM is available in the recent review (Ng et al., 2011). The HR-ToF-AMS and  
134 ACSM were calibrated every month following the standard protocols (Ng et al., 2011; Jayne et al.,  
135 2000).

136

137 An aethalometer (AE-31) (Magee, US) was used for simultaneous detection of refractory black carbon  
138 (BC) with a time resolution of 5 min. In addition, a Scan Mobility Particle Sizer (TSI Inc., US) system  
139 was used to determine the particle number size distribution in the size range 15–615 nm (Stokes  
140 diameter) with a time resolution of 5 min. The stokes diameters of 15–615 nm is converted to  
141 aerodynamic diameters of 22–800 nm, and then PM<sub>0.8</sub> mass concentration can be calculated with the

142 particle density assumed according to the AMS measurement results of species.

143

144 To measure the PM<sub>2.5</sub> mass concentration, we used a Thermo Scientific TEOM 1405–D monitor. The  
145 trace-gas instruments included a 43i sulfur dioxide (SO<sub>2</sub>) analyzer, a 42i nitric oxide (NO)–nitrogen  
146 dioxide (NO<sub>2</sub>)–nitrogen oxide (NO<sub>x</sub>) analyzer, a 49i ozone (O<sub>3</sub>) analyzer, and a 48i carbon monoxide  
147 (CO) analyzer (Thermo Scientific, US). A meteorological station, also located on the roof of the same  
148 building, measured the main meteorological parameters, such as temperature, relative humidity, and  
149 wind speed (see Table 1).

150

## 151 **3 Results and Discussion**

### 152 **3.1 The NSF–SF differences for major air pollutants**

153 The results of observations from 2014 to 2016 appear in Figures S3–S5. Figure 1 shows the averaged  
154 percent changes in the concentrations of major air pollutants of the SF periods relative to the two NSF  
155 periods and Tran. period over 2014–2016. Most of fragments of m/z 44 and m/z 57 are the tracer of  
156 oxygenated organic aerosol and the tracer of primary hydrocarbon organic aerosol (Zhang et al., 2005),  
157 respectively, which are measured by AMS. The notation O<sub>3</sub>–8h refers to the average maximum O<sub>3</sub>  
158 concentration over a continuous diurnal 8 h and PM<sub>0.8–2.5</sub> refers to the difference between the  
159 concentrations of PM<sub>2.5</sub> and PM<sub>0.8</sub>.

160

161 We can divide these air pollutants into three classes based on their percent changes: The group with  
162 the largest drop (hereinafter called “LD”) in concentration includes the aromatics (–50% to –88% for  
163 the various species, see Figure S6), OVOCs (–40% to –85% for the various species, see Figure S6),



164 NO<sub>x</sub>, chloride (Chl), nitrate (NO<sub>3</sub><sup>-</sup>), BC, and m/z 57. The concentrations of these pollutants all  
165 decrease by over 50% during the SF period compared with both the NSF periods. Apparently, the  
166 dominant sources for most of these pollutants are primarily local emissions in the urban scale, such as  
167 combustion sources for BC, m/z 57, and NO<sub>x</sub> (Zhang et al., 2005; Kuhlbusch et al., 1998; Lan et al.,  
168 2011), and vehicle, industrial and solvent use for aromatics (Liu et al., 2008). As detailed in the  
169 following section, the diurnal patterns and relationships with respect to wind speed further confirm the  
170 sources of these pollutants. The dramatic decrease in the ambient concentrations of these species is  
171 consistent with reduction in local anthropogenic activities in Shenzhen during the SF period. The SF  
172 causes a 50% decrease in urban traffic and temporarily closing of almost all local industrial plants. The  
173 nitrate and chloride measured by AMS or ACSM are actually ammonium nitrate (NH<sub>4</sub>NO<sub>3</sub>) and  
174 ammonium chloride (NH<sub>4</sub>Cl), which are typical secondary air pollutants. These are thought to form  
175 via reversible phase equilibria with gaseous ammonia (NH<sub>3</sub>), nitric acid (HNO<sub>3</sub>), and hydrochloric  
176 acid (HCl) (He et al., 2011; Huang et al., 2011; Zhang et al., 2007). Typically, the formation of NH<sub>4</sub>NO<sub>3</sub>  
177 from NO<sub>x</sub> and the reaction between HCl and NH<sub>3</sub> occur quickly in the atmosphere (Stelson and  
178 Seinfeld, 1982; Baek et al., 2004), suggesting that the concentrations of NO<sub>3</sub><sup>-</sup> and Chl in winter in  
179 Shenzhen depend largely on the emission of precursors such as HCl and NO<sub>x</sub>. Therefore, the  
180 significant decline in the ambient concentrations of NO<sub>3</sub><sup>-</sup> and Chl during the SF period and indicates  
181 that their precursors also have local origins, similar to the case for primary pollutants (this is also  
182 supported by the discussion in the following sections). The huge decline in the ambient concentration  
183 of OVOCs during the SF period shows that the source of these pollutants is (i) mainly from local  
184 emissions, including vehicle and industrial emissions (Schauer et al., 1999; Singh et al., 2001) and (ii)  
185 from secondary reactions involving local primary VOCs (Liu et al., 2015). Thus, in the LD group, the

186 significant reduction in local sources of pollutants strongly impacts the concentration of air pollutants.  
187

188 The pollutants in the next group undergo a medium drop in concentration during the SF period  
189 (hereinafter called “MD”). These are PM<sub>2.5</sub>, NR-PM<sub>1</sub>, PM<sub>0.8</sub>, organic aerosol, m/z 44, sulfate (SO<sub>4</sub><sup>2-</sup>),  
190 ammonium (NH<sub>4</sub><sup>+</sup>), isoprene, acetonitrile, DMS, and carbon monoxide (CO), and their percent change  
191 varies from -20% to -55% when comparing the SF periods to the NSFT and NSF<sub>M</sub> periods. The  
192 species in this group are either typical regional air pollutants mostly from beyond the urban scale, such  
193 as CO, which has a long lifetime and is a tracer for combustion sources, acetonitrile from rural biomass  
194 burning (de Gouw et al., 2003; Le Breton et al., 2013), m/z 44 representing secondary organic aerosols,  
195 SO<sub>4</sub><sup>2-</sup> from SO<sub>2</sub> oxidation (He et al., 2011; Huang et al., 2011), or typical tracers mainly emitted by  
196 natural sources, such as isoprene from vegetation (Guenther et al., 1995) and DMS from marine source  
197 (Dacey and Wakeham, 1986). In winter, the northeastern monsoon prevails in the PRD and transports  
198 significant amounts of various air pollutants from the northern inland, increasing air pollution of the  
199 PRD to the highest levels through the year (Huang et al., 2014). In particular, the small drop in CO  
200 concentration during the SF period puts it in this group and indicates that the contribution to regional  
201 air pollution does not decrease significantly during the SF period. Note that, the significant declines of  
202 the concentrations of isoprene and DMS imply that they have anthropogenic sources, which will be  
203 supported in the following sections. The other air pollutants in this group are the reflection of the  
204 overall effect of the reduction of relevant air pollutants: OA is the whole of the two types of organic  
205 aerosol represented by m/z 44 and m/z 57, NH<sub>4</sub><sup>+</sup> is represented by SO<sub>4</sub><sup>2-</sup>, NO<sub>3</sub><sup>-</sup> and Chl, and NR-PM<sub>1</sub>  
206 is the sum of all species measured by AMS or ACSM (their average chemical compositions during  
207 different periods are shown in Figure S3–S5).

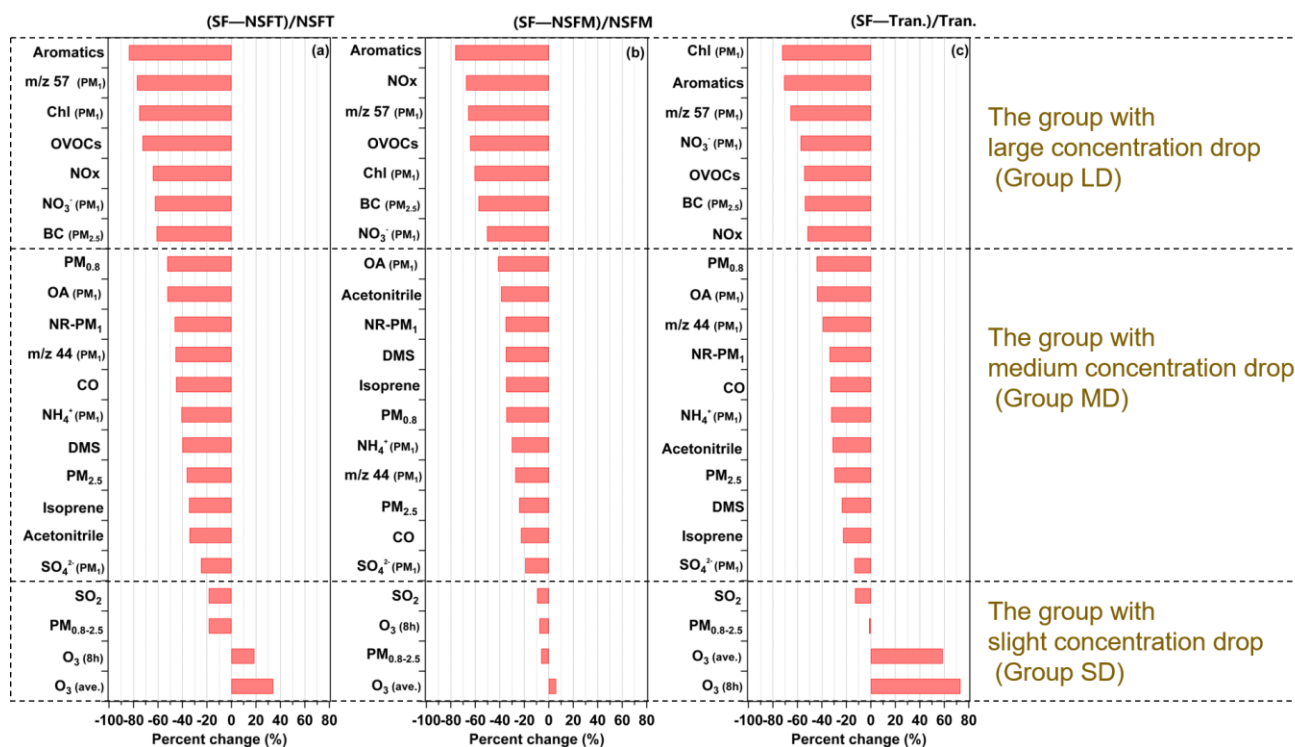
208 The group of pollutants with smallest decrease in concentration (hereinafter called “SD”) includes SO<sub>2</sub>  
209 and PM<sub>0.8–2.5</sub>, and O<sub>3</sub> (8h) in the case of comparison with NSF. The magnitude of the average percent  
210 change is less than 20% relative to the two NSF periods. It is interesting to note that there was even  
211 concentration increase in other O<sub>3</sub>-related cases. The average concentration of SO<sub>2</sub> was only 2.8 ppbv  
212 in Shenzhen in 2015 (<http://www.szhec.gov.cn/>), which is much lower than that in Beijing (4.7 ppbv)  
213 and elsewhere in China (<http://www.zhb.gov.cn/>). This result is partly attributed to the negligible coal  
214 consumption in Shenzhen, which instead relies mainly on natural gas and liquefied petroleum gas  
215 (Shenzhen Yearbook of Statistics, 2015). The emission inventory indicates that power plants and  
216 international marine container vessels are the dominant source of SO<sub>2</sub> in Shenzhen (Wang et al., 2009;  
217 Zheng et al., 2009b). According to official statistics, the Shenzhen port piloted 401, 568, and 521 ships  
218 during the SF period in the years 2014–2016, respectively, which is quite similar to numbers for the  
219 NSF periods (<http://www.pilot.com.cn>). As infrastructure, power plants are not fully shut down during  
220 SF. On the other hand, a piece of evidence for the regional origin of SO<sub>2</sub> is from the newly established  
221 356 m meteorological and environmental monitoring iron tower in Shenzhen. The ambient SO<sub>2</sub>  
222 concentrations were similar at the highest platform (ave.=7.4 ppbv@325 m) and the lowest platform  
223 (ave.=7.2 ppbv@60 m) during January–February, 2017, indicating that SO<sub>2</sub> was already well mixed in  
224 the atmosphere and the local contributions should be minor. In contrast, the concentrations of NO<sub>x</sub>,  
225 which belongs to Group LD, had a 56% higher concentration at the lowest platform than at the highest  
226 platform (Zhuang, 2017). The small decrease of SO<sub>2</sub> is thus a reasonable result of the stable emissions  
227 during the SF periods and the primarily regional origin. The small decline of PM<sub>0.8–2.5</sub> during the SF  
228 period suggests that the reduction of more aged particles of larger sizes in PM<sub>2.5</sub> is much lower than  
229 fresher particles of smaller size. This can be also confirmed by particle number concentration (PNC)

230 measurement by SMPS, as shown in Figure 2. The largest difference of the PNC between the SF and  
231 NSFMM periods exists mainly in a smaller size range (20–40 nm), which is recognized as the nucleation  
232 mode or second Aitken mode that represents fresh combustion emission (Ferin et al., 1990). In terms  
233 of chemical composition of  $PM_{0.8-2.5}$ , implications can be found in our previous size distribution  
234 measurement of aerosol chemical composition, using a ten-stage micro orifice uniform deposit  
235 impactor (MOUDI), during the fall to winter in Shenzhen (Lan et al., 2011). The results clearly indicate  
236 that smaller fine particles (e.g., 0.18–0.56  $\mu m$ ) contains relatively more BC ( $BC/SO_4^{2-}=0.83$ ), while  
237 larger fine particles (e.g., 1.0–1.8  $\mu m$ ) contained a higher proportion of  $SO_4^{2-}$  ( $BC/SO_4^{2-}=0.17$ ). The  
238  $SO_4^{2-}$  in  $PM_{2.5}$  in Shenzhen has been well proved to be mostly a regional pollutant, with similar  
239 concentrations at various sites including both urban and rural sites (Huang et al., 2014). Therefore, the  
240 very small decrease of  $PM_{0.8-2.5}$  during SF should be closely related to its enrichment of secondary  
241 regional species like  $SO_4^{2-}$ . Contrary to other pollutants, the concentrations of  $O_3$ , present small  
242 increasing during the SF period (except a little decline when comparing  $O_3$ -8h with the NSFMM period),  
243 which could be attributed to the different drop rates for  $O_3$  precursor species, i.e.  $NO_x$  and VOCs (Qin  
244 et al., 2004), and will be discussed in more detail in section 3.2.

245

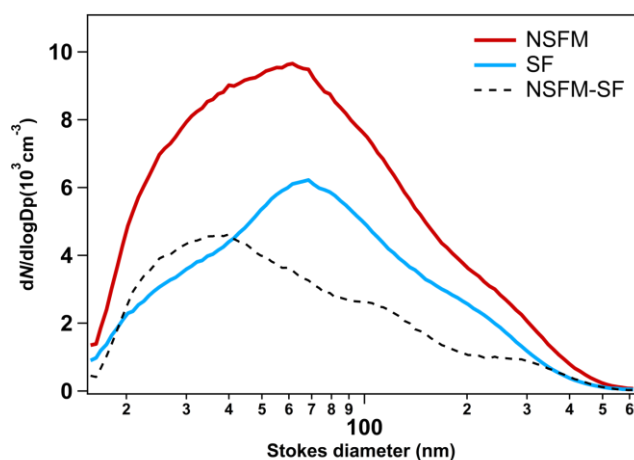
246 The decreasing ratios of various species during SF when compared with the NSFT and NSFMM periods  
247 are similar, which suggests that the meteorological variations might not be the dominant reason for the  
248 species decreasing during SF. This means that the strong decrease in the concentrations of air pollutants  
249 in group LD and MD is mainly due to the abatement of local sources. The larger decline in the SF  
250 period when compared to NSFT than to NSFMM is associated with the lower temperature and stronger  
251 winds from the polluted northwest inland of the PRD during the NSFT period. In addition, the effect

252 of the SF on the concentrations of the various species is almost identical each year (see Figure S7),  
 253 which further confirms that the pollutant concentrations are determined primarily by the activity of the  
 254 sources. In Figure 1, the percent changes of pollutants of the SF periods relative to the Tran. periods  
 255 are also presented, and it is found that the three-group classification defined above is also applicable,  
 256 while the decrease levels are lower. For example, the average decrease percent of Group LD for the  
 257 Tran. period case is 61%, while those for the NSFT and NSFM cases are 71% and 63%, respectively.  
 258 This result is consistent with the fact that the SF travel of people occurred mostly during the seven  
 259 days before and after the SF holidays (<http://sz.gov.cn>), and thus the city became much emptier even  
 260 in the Tran. periods. In order to make a deeper and valid comparison for revealing the SF effect, the  
 261 following discussion will only take the NSFM periods and SF periods for comparative analysis due to  
 262 their more similar meteorology.



263  
 264 **Figure 1.** Percent change in concentrations of major air pollutants during the SF period relative to (a)

265 Tran., (b) NSFT and (c) NSFMT periods averaged over 2014–2016.



266

267 **Figure 2.** Distribution of particle number concentration in the 15–615 nm size range during the SF  
268 and NSFMT periods.

269

### 270 3.2 The diurnal variation of major air pollutants

271 As shown in Figure 3, the diurnal cycles of all LD pollutants (except for the OVOCs) reveal significant  
272 peaks in concentration around 8–9 am in the NSFMT period, which is attributed to the low planetary  
273 boundary layer (PBL) in the morning and local rush hour traffic emissions. The evening rush hour  
274 peak, however, is not apparent for all the species, which is attributed to the higher ambient temperature  
275 and thus the higher PBL at that time than in the morning. During the SF period, the concentrations of  
276 all pollutants are far lower over the entire day. In particular, the rush-hour peaks become much smaller  
277 or disappear altogether, which is consistent with the large reduction in local vehicle emissions during  
278 the SF period. Although the sources of Chl remained uncertain in previous studies (Huang et al., 2011;  
279 Aiken et al., 2008), the maximal reduction (80%) in this pollutant during the morning rush hour during  
280 the SF period implies that local traffic emissions account for a significantly fraction of this pollutant

281 in Shenzhen (Figure 3E). Contrary to other species in this group, the concentration of OVOCs is high  
282 in the daytime and peaks in the morning after the morning rush hour time during the NSF period  
283 (Figure 3D), suggesting that photochemical production and/or daytime industrial activities may be  
284 important sources of OVOCs. The concentrations of different aromatics and OVOCs usually follow  
285 similar diurnal variations (Figure S8).

286

287 The diurnal variations of the MD pollutants are relatively smooth except for two VOCs mainly from  
288 natural sources (isoprene and DMS; see Figures 3L and 3M), which indicates that these pollutants  
289 predominantly come from regional sources and are dispersed more uniformly over a larger scale. The  
290 apparent difference of the diurnal variations of those anthropogenic air pollutants between the SF and  
291 NSF periods also exists in the rush hours (except for acetonitrile; Figure 3J), however, the reduction  
292 in local sources has a relatively weak effect on the overall concentrations of these pollutants.  
293 Acetonitrile, which is a tracer of biomass burning, is more concentrated during the daytime and its  
294 peak concentration occurs after the rush hours during the NSF period (Figure 3J), which is similar  
295 to the result obtained for OVOCs and may be attributed to the influence of daytime anthropogenic  
296 activities, for example, industrial biomass boilers. Isoprene is primarily emitted by vegetation as a  
297 function of light and temperature, so the concentration of this pollutant goes through a broad peak that  
298 spans the daytime hours during both the NSF and SF periods. The percent change in isoprene  
299 concentration between the SF and NSF periods is approximately -40% (Figure 3M), despite the  
300 NSF and SF periods having similar temperature and solar radiation, which implies that the  
301 contribution of anthropogenic sources to isoprene cannot be overlooked in Shenzhen. Many studies  
302 have reported isoprene from vehicle exhaust, especially in cold seasons (Barletta et al., 2005; Borbon

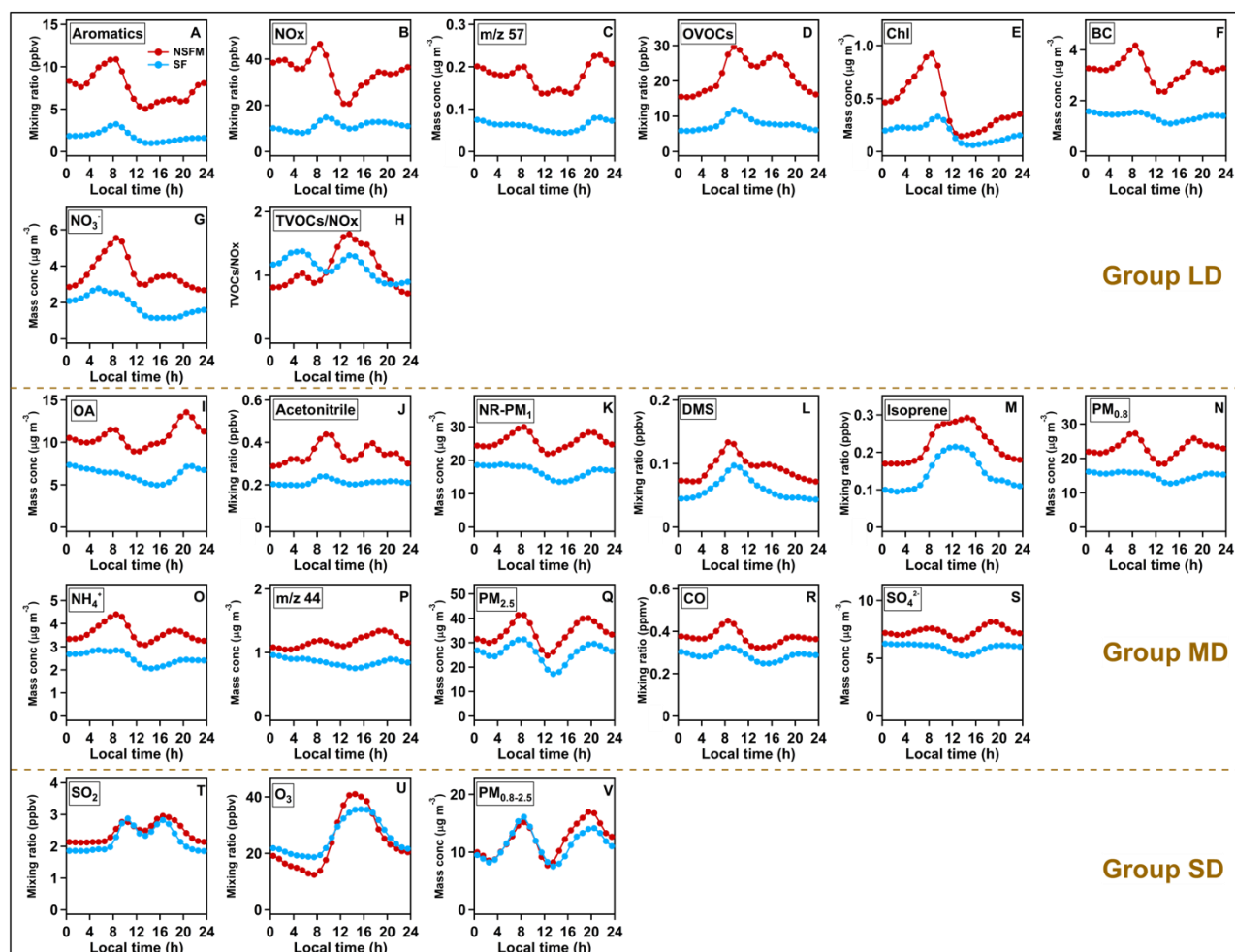
303 et al., 2001). DMS is reported to be a marine tracer (Dacey et al., 1986), its peak concentration occurs  
304 in the morning during both the NSF and SF periods (Figure 3L), which is presumably related to the  
305 minimal PBL. The concentration of DMS decreases by 30%–50% during the SF period, which reflects  
306 the reduced DMS emissions from anthropogenic sources. As reported in the literature, industrial  
307 activities can make significant emissions of DMS (Schafer et al., 2010).

308

309 The diurnal variations of  $PM_{0.8-2.5}$ ,  $SO_2$  and  $O_3$  demonstrated more similar concentrations and trends  
310 in the SF and NSF periods, respectively (Figure 3T–3V). For  $PM_{0.8-2.5}$ , a small difference is found  
311 in the afternoon, which is supposed to be a result of more aged larger particles formed through stronger  
312 photochemical reactions during the NSF period. Though, slight differences appear in  $SO_2$   
313 concentration, mainly during the nighttime when the PBL is low. These data suggest a minor role of  
314 local near-ground  $SO_2$  sources, such as vehicles. Although the daytime peak concentration of  $O_3$  during  
315 the NSF period is slightly greater than that during the SF period, this trend reverses from the evening  
316 to the midmorning hours. Similar phenomena have also been observed in other emission-reduction  
317 studies of urban areas (i.e.,  $O_3$  concentrations are greater on holidays than on non-holidays) (Qin et al.,  
318 2004; Tan et al., 2009). In addition,  $O_3$  concentrations were higher during the 2008 Beijing Olympic  
319 Games (Chou et al., 2011), during which strict controls were imposed. The lower peak concentration  
320 of  $O_3$  in the afternoon (13:00-16:00 LT) during SF suggests that the large reduction on precursors can  
321 also help mitigate the daytime  $O_3$  concentration. However, the  $O_3$  concentration at night during SF  
322 was higher than that during NSF, which could be attributed to the oxidation reaction with NO of  
323 higher concentrations during NSF, producing a titration effect and thus destroying  $O_3$  (Qin et al.,  
324 2004; Tan et al., 2009). As a result, although the reduction in emissions of urban anthropogenic sources



325 leads to a large decline of NO<sub>x</sub> and VOCs, this reduction does not mitigate the average ambient O<sub>3</sub>  
 326 concentration, which implies that the concentration ratio VOCs/NO<sub>x</sub> play an important role in  
 327 controlling O<sub>3</sub> concentration.



328  
 329 **Figure 3.** Diurnal variations in concentrations of major air pollutants at PKUSZ site over the SF  
 330 (blue dots) and NSFM (red dots) periods.

331

### 332 3.3 Influence of wind on observed air pollutants

333 Wind plays a crucial role in the dilution and transport of air pollution. The wind field patterns are quite  
 334 similar between the SF and NSFM periods (Figure S2). In general, the concentrations of LD air

335 pollutants depend strongly on wind speed during the NSF<sub>M</sub> period, whereas this dependence becomes  
336 much weaker during the SF period (Figure 4). The difference in the concentration of LD air pollutants  
337 (including various aromatics and OVOCs, see Figure S9) between the NSF<sub>M</sub> and SF periods is  
338 maximal (50%–80%) under conditions of low wind speeds (<1 m/s) because local pollution can more  
339 easily accumulate under these conditions. These results confirm that the concentration of air pollutants  
340 mainly from local sources is strongly reduced during in the SF period.

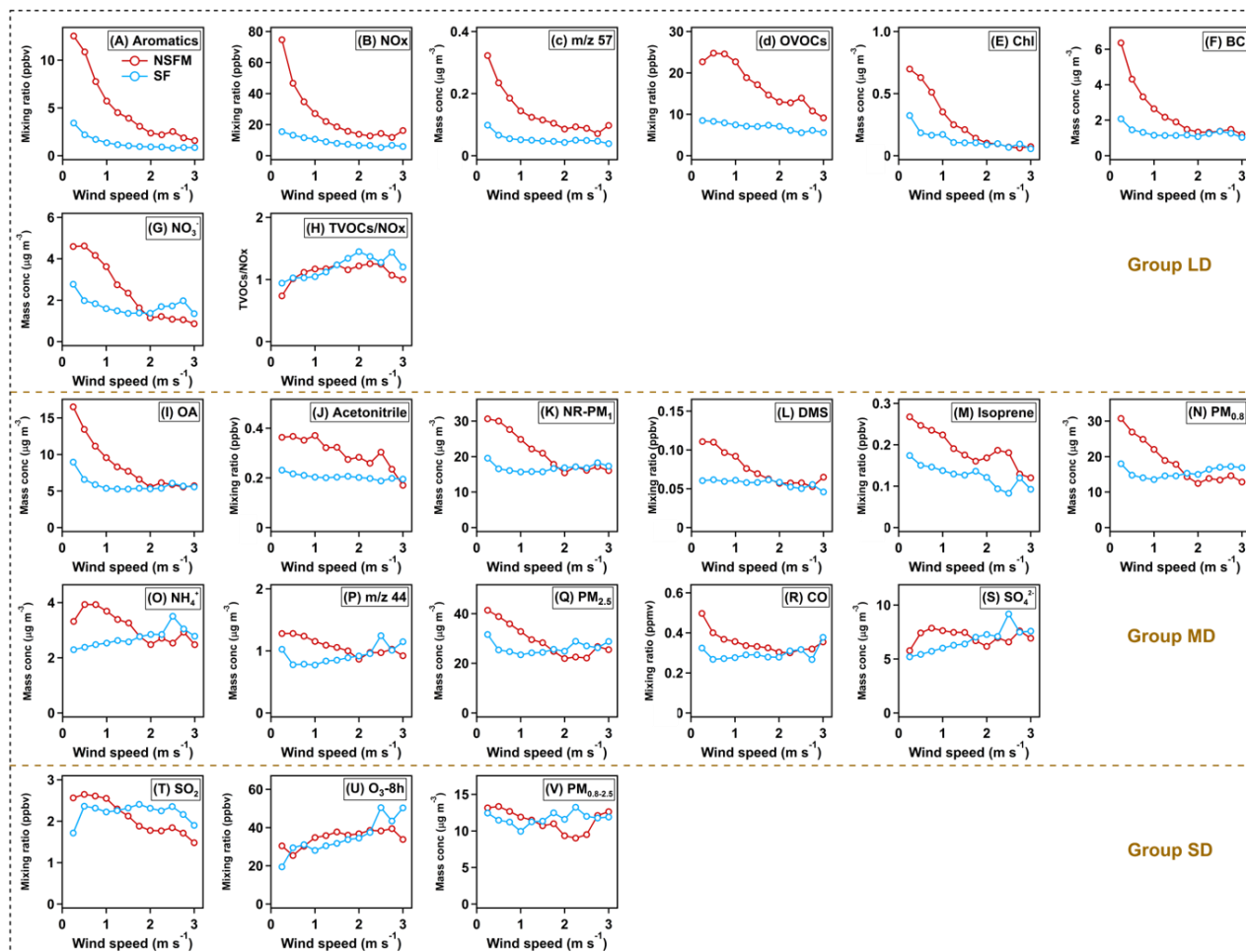
341

342 Compared with the LD pollutants, the concentrations of CO, SO<sub>4</sub><sup>2-</sup>, m/z 44, isoprene, DMS, and  
343 acetonitrile do not vary significantly with wind speed during the NSF<sub>M</sub> period, providing further  
344 evidence that these pollutants primarily come from regional or natural sources and are consequently  
345 more evenly distributed in the atmosphere.

346

347 In the Group SD, SO<sub>2</sub> is generally little influenced by wind speed during the SF period, while some  
348 higher concentrations appeared under low wind speeds during the NSF<sub>M</sub> period, indicating again small  
349 contribution of urban local sources to SO<sub>2</sub>. The fluctuation of PM<sub>0.8-2.5</sub> both in the SF and NSF<sub>M</sub>  
350 periods does not reveal a clear relationship with wind speed, suggesting again it is not a typical locally  
351 emitted air pollutant. The variations of O<sub>3-8h</sub> display the opposite trend to other air pollutants both in  
352 the SF and NSF<sub>M</sub> periods, growing smoothly as wind speed increases, which could be possibly  
353 attributed to more regional transport and/or the higher VOCs/NO<sub>x</sub> ratio under high wind speeds  
354 (Figure 4H). Note that, when the proportion of regional transport relative to local emission becomes  
355 bigger under higher wind speeds, the concentrations of NO<sub>3</sub><sup>-</sup>, SO<sub>4</sub><sup>2-</sup>, m/z 44, PM<sub>0.8-2.5</sub>, and O<sub>3-8h</sub> are  
356 even slightly higher in the SF period than in the NSF<sub>M</sub> period, implying that regional photochemical

357 production during the SF period is not weakened.



358  
 359 **Figure 4.** Concentrations of major air pollutants as a function of wind speed during the SF and  
 360 NSFm periods.

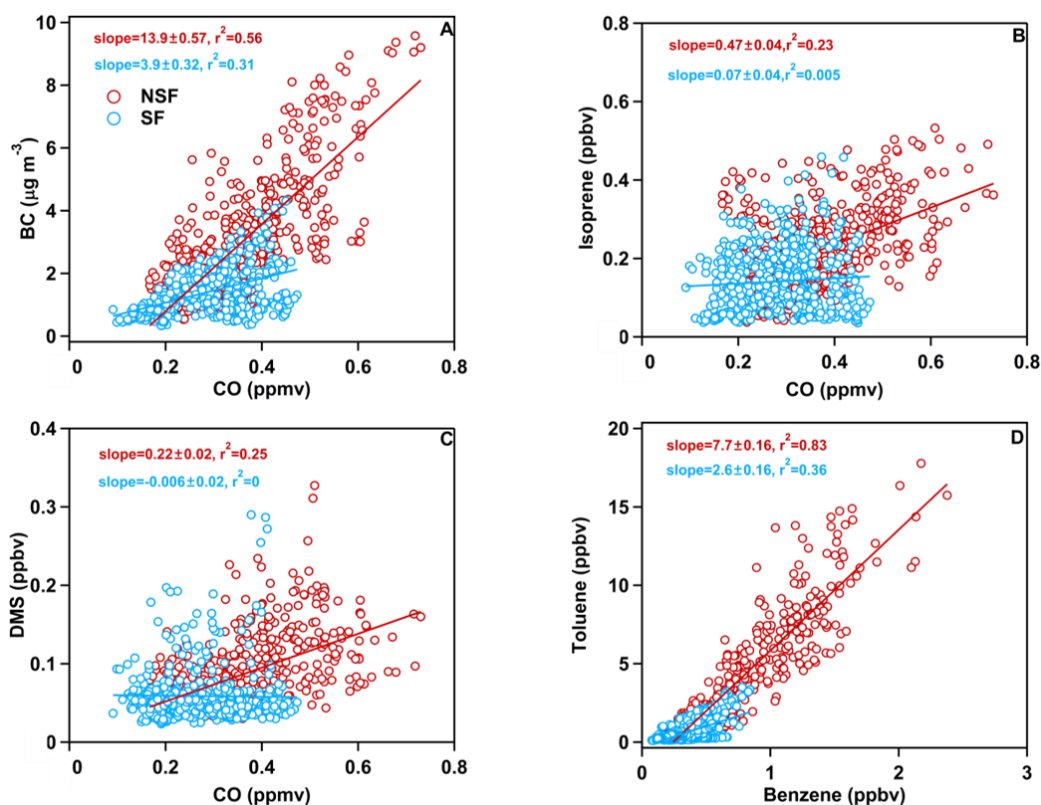
361  
 362 **3.4 Emission ratio analysis**

363 Several groups of special correlations were applied to analyze the source characteristics of air  
 364 pollutants in Figure 5. CO and BC are both products of incomplete combustion (Subramanian et al.,  
 365 2010), but gaseous CO can travel farther because of its longer atmospheric lifetime (approximately a  
 366 month for CO vs a week for BC) (Khalil et al., 1990; Ogren et al., 1983). As shown in Figure 5A, the

367 correlation coefficient and slope between BC and CO during the NSFPM period ( $r^2 = 0.56$ , slope = 13.9)  
368 is greater than during the SF period ( $r^2 = 0.31$ , slope = 3.9), suggesting that local combustion sources  
369 make a much greater contribution during the NSFPM period, but decline significantly during the SF  
370 period (He et al., 2011). The concentrations of isoprene and DMS, are not correlated with CO during  
371 the SF, whereas their correlation with CO is non-negligible during the NSFPM period (Figures 5B and  
372 5C), suggesting again that these pollutants have an anthropogenic source during the NSFPM period.

373

374 The toluene/benzene ratio can be used to estimate the contribution of traffic emissions (Schneider et  
375 al., 2005). Generally, a value of 1.2–3 is found to be characteristic of vehicular emission in many urban  
376 areas (Nelson et al., 1984; Wang et al., 2002; Araizaga et al., 2013). The lower ratio of toluene to  
377 benzene (ave.=2.6) in the SF period suggests that the dominant source is vehicle emission. This ratio  
378 in the NSFPM period, however, is much higher (ave.=7.7), indicating more complicated sources of  
379 VOCs like huge amount of toluene solvent usage in industrial activities in PRD (Barletta et al., 2005,  
380 2008; Chan et al., 2006). This finding is well consistent with the temporary closure of industrial plants  
381 in the SF period, which leads to little toluene emission.



382

383 **Figure 5.** Correlation between air pollutants (A) BC and CO (B) isoprene and CO, (C) DMS and  
 384 CO, and (D) toluene and benzene during the SF (blue circles) and the NSF (red circles) periods.

385

### 386 3.5 Conclusions

387 This study uses the SF in Shenzhen to investigate how the urban air quality reacts to significant,  
 388 temporary reductions in emission. During the winters of 2014 to 2016, the air quality was observed  
 389 continuously at Peking University Shenzhen Graduate School, from which we obtained the percent  
 390 change in the concentrations of various air pollutants during the SF periods with respect to the  
 391 comparable NSF periods. The analysis of these data shows that, despite meteorological variations, the  
 392 Spring Festival clearly and consistently influences the urban concentrations of various air pollutants.  
 393 The air pollutants can be divided into three groups: the large-decrease (LD) pollutants are those with

394 a percent change in concentration of  $-50\%$  to  $-80\%$  during the SF period and include aromatics,  $\text{NO}_x$ ,  
395  $m/z$  57, OVOCs, Chl, BC, and  $\text{NO}_3^-$ . These results are consistent with the variation in urban emission  
396 sources during the SF, suggesting that these pollutants are mostly directly locally emitted or formed  
397 from secondary reactions between locally emitted pollutants. The medium-decrease (MD) pollutants  
398 are  $\text{PM}_{2.5}$ ,  $\text{NR-PM}_1$ ,  $\text{PM}_{0.8}$ , organic aerosol,  $m/z$  44,  $\text{SO}_4^{2-}$ ,  $\text{NH}_4^+$ , isoprene, acetonitrile, DMS, and  
399 CO; the concentrations of these pollutants decrease by 20% to 55% during the SF, which indicates that  
400 the extreme reduction in urban emissions during the SF period has limited effect on air pollutants  
401 mostly from regional or natural sources. Finally, the slight-decrease (SD) pollutants include  $\text{SO}_2$ ,  
402  $\text{PM}_{0.8-2.5}$ , and  $\text{O}_3$ . The average percent change in the concentrations of these pollutants during the SF  
403 period is less than 20%, which indicates that a significant reduction in urban emissions does not  
404 significantly affect their concentration. Of particular interest is the origin of  $\text{PM}_{0.8-2.5}$ , which is almost  
405 completely regional.

406

407 The results of this study show that the extreme reductions in urban emissions of Shenzhen only affects  
408 the concentration of smaller fresh particles, such as  $\text{PM}_{0.8}$ , whereas the reduction of  $\text{PM}_{2.5}$  is only  
409 slightly affected because of the weak influence on aged, larger particles such as  $\text{PM}_{0.8-2.5}$ . The  
410 concentrations of  $\text{SO}_4^{2-}$  and secondary organic aerosols are hardly affected by local reductions in  
411 emissions. Therefore, reducing the emissions of  $\text{SO}_2$  and VOCs on a regional scale is critical for  
412 reducing their concentrations and achieving the goal of reducing concentrations of  $\text{PM}_{2.5}$ , at least for  
413 South China. On the other hand,  $\text{O}_3$  has recently become an increasingly important air pollutant in  
414 China, especially in the PRD. However, the large reduction of  $\text{O}_3$  precursors ( $\text{NO}_x$  and VOCs) during  
415 the SF period only lead to small variation of  $\text{O}_3$  concentrations. Consequently, further investigations

416 are required to control not only the emissions of VOCs and NO<sub>x</sub> but also their concentration ratio.

417

## 418 **Acknowledgements**

419 This work was supported by the National Natural Science Foundation of China (U1301234 &  
420 41622304), the Ministry of Science and Technology of China (2014BAC21B03), and the Science and  
421 Technology Plan of Shenzhen Municipality.

422

## 423 **Reference**

424 Aiken, A. C., Decarlo, P. F., Kroll, J. H., Worsnop, D. R., Huffman, J. A., Docherty, K. S., Ulbrich, I.  
425 M., Mohr, C., Kimmel, J. R., Sueper, D., Sun, Y., Zhang, Q., Trimborn, A., Northway, M., Ziemann,  
426 P. J., Canagaratna, M. R., Onasch, T. B., Alfarra, M. R., Prevot, A. S. H., Dommen, J., Duplissy, J.,  
427 Metzger, A., Baltensperger, U., and Jimenez, J. L.: O/C and OM/OC ratios of primary, secondary,  
428 and ambient organic aerosols with high-resolution time-of-flight aerosol mass spectrometry,  
429 *Environ. Sci. Technol.*, 42, 4478-4485, doi:10.1021/es703009q, 2008.

430 Araizaga, A. E., Mancilla, Y., and Mendoza, A.: Volatile Organic Compound Emissions from Light-  
431 Duty Vehicles in Monterrey, Mexico: a Tunnel Study, *Int. J. Environ. Res.*, 7, 277-292, 2013.

432 Baek, B. H., Aneja, V. P., and Tong, Q. S.: Chemical coupling between ammonia, acid gases, and fine  
433 particles, *Environ. Pollut.*, 129, 89-98, doi:10.1016/j.envpol.2003.09.022, 2004.

434 Barletta, B., Meinardi, S., Rowland, F. S., Chan, C. Y., Wang, X. M., Zou, S. C., Chan, L. Y., and Blake,  
435 D. R.: Volatile organic compounds in 43 Chinese cities, *Atmos. Environ.*, 39, 5979-5990,  
436 doi:10.1016/j.atmosenv.2005.06.029, 2005.

437 Barletta, B., Meinardi, S., Simpson, I. J., Zou, S. C., Rowland, F. S., and Blake, D. R.: Ambient mixing  
438 ratios of nonmethane hydrocarbons (NMHCs) in two major urban centers of the Pearl River Delta  
439 (PRD) region: Guangzhou and Dongguan, *Atmos. Environ.*, 42, 4393-4408,  
440 doi:10.1016/j.atmosenv.2008.01.028, 2008.

441 Borbon, A., Fontaine, H., Veillerot, M., Locoge, N., Galloo, J. C., and Guillermo, R.: An investigation

442 into the traffic-related fraction of isoprene at an urban location, *Atmos. Environ.*, 35, 3749-3760,  
443 doi:10.1016/S1352-2310(01)00170-4, 2001.

444 Canagaratna, M. R., Jayne, J. T., Jimenez, J. L., Allan, J. D., Alfarra, M. R., Zhang, Q., Onasch, T. B.,  
445 Drewnick, F., Coe, H., Middlebrook, A., Delia, A., Williams, L. R., Trimborn, A. M., Northway, M.  
446 J., DeCarlo, P. F., Kolb, C. E., Davidovits, P., and Worsnop, D. R.: Chemical and microphysical  
447 characterization of ambient aerosols with the aerodyne aerosol mass spectrometer, *Mass Spectrom.*  
448 *Rev.*, 26, 185-222, doi:10.1002/mas.20115, 2007.

449 Chan, L. Y., Chu, K. W., Zou, S. C., Chan, C. Y., Wang, X. M., Barletta, B., Blake, D. R., Guo, H., and  
450 Tsai, W. Y.: Characteristics of nonmethane hydrocarbons (NMHCs) in industrial, industrial-urban,  
451 and industrial-suburban atmospheres of the Pearl River Delta (PRD) region of south China, *J.*  
452 *Geophys. Res.-Atmos.*, 111(D11), D11304, doi:10.1029/2005jd006481, 2006.

453 Chen, C., Sun, Y. L., Xu, W. Q., Du, W., Zhou, L. B., Han, T. T., Wang, Q. Q., Fu, P. Q., Wang, Z. F.,  
454 Gao, Z. Q., Zhang, Q., and Worsnop, D. R.: Characteristics and sources of submicron aerosols above  
455 the urban canopy (260m) in Beijing, China, during the 2014 APEC summit, *Atmos. Chem. Phys.*,  
456 15, 12879–12895, doi:10.5194/acp-15-12879-2015, 2015.

457 Chou, C. C. K., Tsai, C. Y., Chang, C. C., Lin, P. H., Liu, S. C., and Zhu, T.: Photochemical production  
458 of ozone in Beijing during the 2008 Olympic Games, *Atmos. Chem. Phys.*, 11, 9825-9837,  
459 doi:10.5194/acp-11-9825-2011, 2011.

460 Dacey, J. W. H., and Wakeham, S. G.: Oceanic Dimethylsulfide - Production during Zooplankton  
461 Grazing on Phytoplankton, *Science*, 233, 1314-1316, doi:10.1126/science.233.4770.1314, 1986.

462 de Gouw, J. A., Warneke, C., Parrish, D. D., Holloway, J. S., Trainer, M., and Fehsenfeld, F. C.:  
463 Emission sources and ocean uptake of acetonitrile (CH<sub>3</sub>CN) in the atmosphere, *J. Geophys. Res.-*  
464 *Atmos.*, 108, doi:10.1029/2002jd002897, 2003.

465 de Gouw, J., and Warneke, C.: Measurements of volatile organic compounds in the earths atmosphere  
466 using proton-transfer-reaction mass spectrometry, *Mass Spectrom. Rev.*, 26, 223-257,  
467 doi:10.1002/mas.20119, 2007.

468 Feng, J. L., Sun, P., Hu, X. L., Zhao, W., Wu, M. H., and Fu, J. M.: The chemical composition and  
469 sources of PM<sub>2.5</sub> during the 2009 Chinese New Year's holiday in Shanghai, *Atmos. Res.*, 118, 435-  
470 444, doi:10.1016/j.atmosres.2012.08.012, 2012.

471 Ferin, J., Oberdorster, G., Penney, D. P., Soderholm, S. C., Gelein, R., and Piper, H. C.: Increased



472 Pulmonary Toxicity of Ultrafine Particles .1. Particle Clearance, Translocation, Morphology, J.  
473 Aerosol Sci., 21, 381-384, doi:10.1016/0021-8502(90)90064-5, 1990.

474 Guenther, A., Hewitt, C. N., Erickson, D., Fall, R., Geron, C., Graedel, T., Harley, P., Klinger, L.,  
475 Lerda, M., McKay, W. A., Pierce, T., Scholes, B., Steinbrecher, R., Tallamraju, R., Taylor, J., and  
476 Zimmerman, P.: A Global-Model Of Natural Volatile Organic-Compound Emissions, J. Geophys.  
477 Res.-Atmos., 100, 8873-8892, doi:10.1029/94jd02950, 1995.

478 Guo, S., Hu, M., Zamora, M. L., Peng, J. F., Shang, D. J., Zheng, J., Du, Z. F., Wu, Z., Shao, M., Zeng,  
479 L. M., Molina, M. J., and Zhang, R. Y.: Elucidating severe urban haze formation in China, P. Natl.  
480 Acad. Sci. USA, 111, 17373-17378, doi:10.1073/pnas.1419604111, 2014.

481 Hagler, G. S., Bergin, M. H., Salmon, L. G., Yu, J. Z., Wan, E. C. H., Zheng, M., Zeng, L. M., Kiang,  
482 C. S., Zhang, Y. H., Lau, A. K. H., and Schauer, J. J.: Source areas and chemical composition of fine  
483 particulate matter in the Pearl River Delta region of China, Atmos. Environ., 40, 3802-3815,  
484 doi:10.1016/j.atmosenv.2006.02.032, 2006.

485 He, L. Y., Huang, X. F., Xue, L., Hu, M., Lin, Y., Zheng, J., Zhang, R. Y., and Zhang, Y. H.: Submicron  
486 aerosol analysis and organic source apportionment in an urban atmosphere in Pearl River Delta of  
487 China using high-resolution aerosol mass spectrometry, J. Geophys. Res.-Atmos., 116, D12304,  
488 doi:10.1029/2010jd014566, 2011.

489 Huang, R. J., Zhang, Y. L., Bozzetti, C., Ho, K. F., Cao, J. J., Han, Y. M., Daellenbach, K. R., Slowik,  
490 J. G., Platt, S. M., Canonaco, F., Zotter, P., Wolf, R., Pieber, S. M., Brun, E. A., Crippa, M., Ciarelli,  
491 G., Piazzalunga, A., Schwikowski, M., Abbaszade, G., Schnelle-Kreis, J., Zimmermann, R., An, Z.  
492 S., Szidat, S., Baltensperger, U., El Haddad, I., and Prevot, A. S. H.: High secondary aerosol  
493 contribution to particulate pollution during haze events in China, Nature, 514, 218-222,  
494 doi:10.1038/nature13774, 2014.

495 Huang, X. F., Yu, J. Z., He, L. Y., and Yuan, Z. B.: Water-soluble organic carbon and oxalate in aerosols  
496 at a coastal urban site in China: Size distribution characteristics, sources, and formation mechanisms,  
497 J. Geophys. Res.-Atmos., 111, D22212, doi:10.1029/2006jd007408, 2006.

498 Huang, X. F., He, L. Y., Hu, M., Canagaratna, M. R., Sun, Y., Zhang, Q., Zhu, T., Xue, L., Zeng, L. W.,  
499 Liu, X. G., Zhang, Y. H., Jayne, J. T., Ng, N. L., and Worsnop, D. R.: Highly time-resolved chemical  
500 characterization of atmospheric submicron particles during 2008 Beijing Olympic Games using an  
501 Aerodyne High-Resolution Aerosol Mass Spectrometer, Atmos. Chem. Phys., 10, 8933-8945,

502 doi:10.5194/acp-10-8933-2010, 2010.

503 Huang, X. F., He, L. Y., Hu, M., Canagaratna, M. R., Kroll, J. H., Ng, N. L., Zhang, Y. H., Lin, Y., Xue,  
504 L., Sun, T. L., Liu, X. G., Shao, M., Jayne, J. T., and Worsnop, D. R.: Characterization of submicron  
505 aerosols at a rural site in Pearl River Delta of China using an Aerodyne High-Resolution Aerosol  
506 Mass Spectrometer, *Atmos. Chem. Phys.*, 11, 1865-1877, doi:10.5194/acp-11-1865-2011, 2011.

507 Huang, X. F., Xue, L., Tian, X. D., Shao, W. W., Sun, T. L., Gong, Z. H., Ju, W. W., Jiang, B., Hu, M.,  
508 and He, L. Y.: Highly time-resolved carbonaceous aerosol characterization in Yangtze River Delta  
509 of China: Composition, mixing state and secondary formation, *Atmos. Environ.*, 64, 200-207,  
510 doi:10.1016/j.atmosenv.2012.09.059, 2013.

511 Huang, X. F., Yun, H., Gong, Z. H., Li, X., He, L., Zhang, Y. H., and Hu, M.: Source apportionment  
512 and secondary organic aerosol estimation of PM<sub>2.5</sub> in an urban atmosphere in China, *Sci. China  
513 Earth Sci.*, 57, 1352-1362, doi:10.1007/s11430-013-4686-2, 2014.

514 Jayne, J. T., Leard, D. C., Zhang, X. F., Davidovits, P., Smith, K. A., Kolb, C. E., and Worsnop, D. R.:  
515 Development of an aerosol mass spectrometer for size and composition analysis of submicron  
516 particles, *Aerosol Sci. Tech.*, 33, 49-70, doi:10.1080/027868200410840, 2000.

517 Jiang, J. B., Jin, W., Yang, L. L., Feng, Y., Chang, Q., Li, Y. Q., and Zhou, J. B.: The Pollution  
518 Characteristic of VOCs of Ambient Air in Winter in Shijiazhang, *Environmental Monitoring in  
519 China*, 31, 2015 (in Chinese).

520 Khalil, M. A. K., and Rasmussen, R. A.: The Global Cycle of Carbon-Monoxide-Trends And Mass  
521 Balance, *Chemosphere*, 20, 227-242, doi: 10.1016/0045-6535(90)90098-E, 1990.

522 Kuhlbusch, T. A. J.: Black carbon and the carbon cycle, *Science*, 280, 1903-1904,  
523 doi:10.1126/science.280.5371.1903, 1998.

524 Lan, Z. J., Chen, D. L., Li, X. A., Huang, X. F., He, L. Y., Deng, Y. G., Feng, N., and Hu, M.: Modal  
525 characteristics of carbonaceous aerosol size distribution in an urban atmosphere of South China,  
526 *Atmos. Res.*, 100, 51-60, doi:10.1016/j.atmosres.2010.12.022, 2011.

527 Le Breton, M., Bacak, A., Muller, J. B. A., O'Shea, S. J., Xiao, P., Ashfold, M. N. R., Cooke, M. C.,  
528 Batt, R., Shallcross, D. E., Oram, D. E., Forster, G., Bauguitte, S. J. B., and Percival, C. J.: Airborne  
529 hydrogen cyanide measurements using a chemical ionisation mass spectrometer for the plume  
530 identification of biomass burning forest fires, *Atmos. Chem. Phys.*, 13, 9217-9232, doi:10.5194/acp-  
531 13-9217-2013, 2013.

532 Li, P. F., Yan, R. C., Yu, S. C., Wang, S., Liu, W. P., and Bao, H. M.: Reinstatement of regional transport of  
533 PM<sub>2.5</sub> as a major cause of severe haze in Beijing, *P. Natl. Acad. Sci. USA*, 112, E2739-E2740,  
534 doi:10.1073/pnas.1502596112, 2015.

535 Liu, Y., Shao, M., Lu, S. H., Chang, C. C., Wang, J. L., and Fu, L. L.: Source apportionment of ambient  
536 volatile organic compounds in the Pearl River Delta, China: Part II, *Atmos. Environ.*, 42, 6261-6274,  
537 doi:10.1016/j.atmosenv.2008.02.027, 2008.

538 Liu, Y., Yuan, B., Li, X., Shao, M., Lu, S., Li, Y., Chang, C. C., Wang, Z., Hu, W., Huang, X., He, L.,  
539 Zeng, L., Hu, M., and Zhu, T.: Impact of pollution controls in Beijing on atmospheric oxygenated  
540 volatile organic compounds (OVOCs) during the 2008 Olympic Games: observation and modeling  
541 implications, *Atmos. Chem. Phys.*, 15, 3045-3062, doi:10.5194/acp-15-3045-2015, 2015.

542 Louie, P. K. K., Watson, J. G., Chow, J. C., Chen, A., Sin, D. W. M., and Lau, A. K. H.: Seasonal  
543 characteristics and regional transport of PM<sub>2.5</sub> in Hong Kong, *Atmos. Environ.*, 39, 1695-1710,  
544 doi:10.1016/j.atmosenv.2004.11.017, 2005.

545 Nelson, P. F., and Quigley, S. M.: The Hydrocarbon Composition Of Exhaust Emitted From Gasoline  
546 Fueled Vehicles, *Atmos. Environ.*, 18, 79-87, doi:10.1016/0004-6981(84)90230-0, 1984.

547 Ng, N. L., Herndon, S. C., Trimborn, A., Canagaratna, M. R., Croteau, P. L., Onasch, T. B., Sueper, D.,  
548 Worsnop, D. R., Zhang, Q., Sun, Y. L., and Jayne, J. T.: An Aerosol Chemical Speciation Monitor  
549 (ACSM) for Routine Monitoring of the Composition and Mass Concentrations of Ambient Aerosol,  
550 *Aerosol Sci. Tech.*, 45, 780-794, 2011.

551 Ogren, J. A., and Charlson, R. J.: Elemental Carbon in the Atmosphere-Cycle and Lifetime, *Tellus B.*,  
552 35, 241-254, 1983.

553 Parrish, D. D., and Zhu, T.: Clean Air for Megacities, *Science*, 326, 674-675,  
554 doi:10.1126/science.1176064, 2009.

555 Qin, Y., Tonnesen, G. S., and Wang, Z.: Weekend/weekday differences of ozone, NO<sub>x</sub>, CO, VOCs,  
556 PM<sub>10</sub> and the light scatter during ozone season in southern California, *Atmos. Environ.*, 38, 3069-  
557 3087, doi:10.1016/j.atmosenv.2004.01.035, 2004.

558 Schafer, H., Myronova, N., and Boden, R.: Microbial degradation of dimethylsulphide and related C-  
559 1-sulphur compounds: organisms and pathways controlling fluxes of sulphur in the biosphere, *J.*  
560 *Exp. Bot.*, 61, 315-334, doi:10.1093/jxb/erp355, 2010.

561 Schauer, J. J., Kleeman, M. J., Cass, G. R., and Simoneit, B. R. T.: Measurement of emissions from air

562 pollution sources. 2. C-1 through C-30 organic compounds from medium duty diesel trucks, *Environ.*  
563 *Sci. Technol.*, 33, 1578-1587, doi:10.1021/Es980081n, 1999.

564 Schneider, J., Hock, N., Weimer, S., and Borrmann, S.: Nucleation particles in diesel exhaust:  
565 Composition inferred from in situ mass spectrometric analysis, *Environ. Sci. Technol.*, 39, 6153-  
566 6161, doi:10.1021/es049427m, 2005.

567 Shi, G. L., Liu, G. R., Tian, Y. Z., Zhou, X. Y., Peng, X., and Feng, Y. C.: Chemical characteristic and  
568 toxicity assessment of particle associated PAHs for the short-term anthropogenic activity event:  
569 During the Chinese New Year's Festival in 2013, *Sci. Total Environ.*, 482, 8-14,  
570 doi:10.1016/j.scitotenv.2014.02.107, 2014.

571 Singh, H., Chen, Y., Staudt, A., Jacob, D., Blake, D., Heikes, B., and Snow, J.: Evidence from the  
572 Pacific troposphere for large global sources of oxygenated organic compounds, *Nature*, 410, 1078-  
573 1081, doi:10.1038/35074067, 2001.

574 Stelson, A. W., and Seinfeld, J. H.: Relative-Humidity And Temperature-Dependence Of the  
575 Ammonium-Nitrate Dissociation-Constant, *Atmos. Environ.*, 16, 983-992, doi:10.1016/0004-  
576 6981(82)90184-6, 1982.

577 Subramanian, R., Kok, G. L., Baumgardner, D., Clarke, A., Shinozuka, Y., Campos, T. L., Heizer, C.  
578 G., Stephens, B. B., de Foy, B., Voss, P. B., and Zaveri, R. A.: Black carbon over Mexico: the effect  
579 of atmospheric transport on mixing state, mass absorption cross-section, and BC/CO ratios, *Atmos.*  
580 *Chem. Phys.*, 10, 219-237, doi:10.5194/acp-10-219-2010, 2010.

581 Sun, Y. L., Wang, Z. F., Fu, P. Q., Yang, T., Jiang, Q., Dong, H. B., Li, J., and Jia, J. J.: Aerosol  
582 composition, sources and processes during wintertime in Beijing, China, *Atmos. Chem. Phys.*, 13,  
583 4577–4592, doi:10.5194/acp-13-4577-2013, 2013.

584 Sun, Y. L., Wang, Z. F., Du, W., Zhang, Q., Wang, Q. Q., Fu, P. Q., Pan, X. L., Li, J., Jayne, J., and  
585 Worsnop, D. R.: Long-term real-time measurements of aerosol particle composition in Beijing,  
586 China: seasonal variations, meteorological effects, and source analysis, *Atmos. Chem. Phys.*, 15,  
587 10149-10165, doi:10.5194/acp-15-10149-2015, 2015.

588 Sun, Y. L., Wang, Z., Wild, O., Xu, W., Chen, C., Fu, P., Du, W., Zhou, L., Zhang, Q., Han, T., Wang,  
589 Q., Pan, X., Zheng, H., Li, J., Guo, X., Liu, J., and Worsnop, D. R.: “APEC Blue”: Secondary  
590 Aerosol Reductions from Emission Controls in Beijing, *Sci. Rep.*, 6, 20668, doi:10.1038/srep20668,  
591 2016.

592 Tan, P. H., Chou, C., Liang, J. Y., Chou, C. C. K., and Shiu, C. J.: Air pollution "holiday effect" resulting  
593 from the Chinese New Year, *Atmos. Environ.*, 43, 2114-2124, doi:10.1016/j.atmosenv.2009.01.037,  
594 2009.

595 Wang, S.; Chai, F.; Xia, G.; Zhang, H.; Zhang, M.; Xue, Z.; Source Apportionment and Characteristics  
596 of SO<sub>2</sub> in Shenzhen City. *Res. Environ. Sci.*, 10 (22), 1128–1133, 2009 (in Chinese).

597 Wang, T., Nie, W., Gao, J., Xue, L. K., Gao, X. M., Wang, X. F., Qiu, J., Poon, C. N., Meinardi, S.,  
598 Blake, D., Wang, S. L., Ding, A. J., Chai, F. H., Zhang, Q. Z., and Wang, W. X.: Air quality during  
599 the 2008 Beijing Olympics: secondary pollutants and regional impact, *Atmos. Chem. Phys.*, 10,  
600 7603-7615, doi:10.5194/acp-10-7603-2010, 2010.

601 Wang, X. M., Sheng, G. Y., Fu, J. M., Chan, C. Y., Lee, S. G., Chan, L. Y., and Wang, Z. S.: Urban  
602 roadside aromatic hydrocarbons in three cities of the Pearl River Delta, People's Republic of China,  
603 *Atmos. Environ.*, 36, 5141-5148, doi:10.1016/S1352-2310(02)00640-4, 2002.

604 Xu, H. M., Tao, J., Ho, S. S. H., Ho, K. F., Cao, J. J., Li, N., Chow, J. C., Wang, G. H., Han, Y. M.,  
605 Zhang, R. J., Watson, J. G., and Zhang, J. Q.: Characteristics of fine particulate non-polar organic  
606 compounds in Guangzhou during the 16th Asian Games: Effectiveness of air pollution controls,  
607 *Atmos. Environ.*, 76, 94-101, doi:10.1016/j.atmosenv.2012.12.037, 2013.

608 Zhang, L., Shao, J. Y., Lu, X., Zhao, Y. H., Hu, Y. Y., Henze, D. K., Liao, H., Gong, S. L., and Zhang,  
609 Q.: Sources and Processes Affecting Fine Particulate Matter Pollution over North China: An Adjoint  
610 Analysis of the Beijing APEC Period, *Environ. Sci. Technol.*, 50, 8731-8740,  
611 doi:10.1021/acs.est.6b03010, 2016.

612 Zhang, Q., Worsnop, D. R., Canagaratna, M. R., and Jimenez, J. L.: Hydrocarbon-like and oxygenated  
613 organic aerosols in Pittsburgh: insights into sources and processes of organic aerosols, *Atmos. Chem.*  
614 *Phys.*, 5, 3289-3311, 2005.

615 Zhang, Q., Jimenez, J. L., Worsnop, D. R., and Canagaratna, M.: A case study of urban particle acidity  
616 and its influence on secondary organic aerosol, *Environ. Sci. Technol.*, 41, 3213-3219,  
617 doi:10.1021/es061812j, 2007.

618 Zhang, Y. H., Hu, M., Zhong, L. J., Wiedensohler, A., Liu, S. C., Andreae, M. O., Wang, W., and Fan,  
619 S. J.: Regional Integrated Experiments on Air Quality over Pearl River Delta 2004 (PRIDE-  
620 PRD2004): Overview, *Atmos. Environ.*, 42, 6157-6173, doi:10.1016/j.atmosenv.2008.03.025, 2008.

621 Zhao, J., Du, W. J., Zhang, Y. J., Wang, Q. Q., Chen, C., Xu, W. Q., Han, T. T., Wang, Y. Y., Fu, P. Q.,

622 Wang, Z. F., Li, Z. S., and Sun, Y. L.: Insights into aerosol chemistry during the 2015 China victory  
623 day parade: results from simultaneous measurements at ground level and 260 m in Beijing, *Atmos.*  
624 *Chem. Phys.*, 17, 1-29, doi:10.5194/acp-17-3215-2017, 2016.

625 Zheng, J. Y., Shao, M., Che, W. W., Zhang, L. J., Zhong, L. J., Zhang, Y. H., and Streets, D.: Speciated  
626 VOC Emission Inventory and Spatial Patterns of Ozone Formation Potential in the Pearl River Delta,  
627 China, *Environ. Sci. Technol.*, 43, 8580-8586, doi:10.1021/es901688e, 2009a.

628 Zheng, J., Zhang, L., Che, W., Zheng, Z., and Yin, S.: A highly resolved temporal and spatial air  
629 pollutant emission inventory for the Pearl River Delta region, China and its uncertainty assessment,  
630 *Atmos. Environ.*, 43, 5112-5122, 2009b.

631 Zhuang, X.: Regional distribution characteristics and vertical profiles of complex air pollution in the  
632 Pearl River Delta, Master degree thesis, Peking University, 2017.